Continuously Variable True Time Delay Optical Feeder For Phased Array Antenna Employing Chirped Fiber Gratings

J.L.Corral*, J.Marti, A. Santos, J.M.Fuster, J.Capmany, D.Pastor,

M.J. Cole** , R. Laming**

ETSI Telecomunicacion

Universidad Politecnica de Valencia

Camí de Vera s/n, 46071 València (Spain)

(*) Presently at E.U.Gandia (Valencia)

(**) Optoelectronics Research Centre (Southampton University, Southampton SO17 1BJ, United Kingdom)

Abstract

In this paper we propose and demonstrate a novel approach of true-time delay (TTD) optical feeder for phased-array antennas. A continuously variable TTD is achieved by employing tunable lasers and a wide bandwidth chirped fiber grating as dispersive element. The results show that a very high resolution performance (equivalent to a 6 bit microwave phase shifter) is obtained for a L-band phased-array antenna employing narrow tuning bandwidth lasers with a wavelength stability of 0.005 nm and a 4 nm bandwidth chirped grating with dispersion 835 ps/nm.

I. Introduction

The use of optical fiber in phased arrays has been deeply considered for beamforming and signal distribution [1] as well as for antenna elements synchronization [2]. Its advantages are quite known, such as small size, low losses, lightweight, wide instantaneous bandwidth and immunity to electromagnetic interferences. One key concept in phased array antennas is to find a phase shift element which could show features such as size compactness, low losses, continuous variability, high flexibility and true time delay (thus allowing broad bandwidth squint-free operation). Phase shift selection based on wavelength-switching has been proposed by using dispersive fiber [3-5] to generate relative time delay among the optical wavelengths. Bragg fiber gratings have also been used as wavelength-selective time delay elements [6-8] relying on their wavelength-dependent reflective properties, in such a way that by carefully selecting the grating position each wavelength is associated with a different round-trip time delay. Instead of using several gratings at different discrete positions, we propose a true-time delay optical feeder scheme that employs only one wide bandwidth chirped grating. In this approach since each wavelength is reflected at a different position along the grating length; by tuning the laser wavelength the time delay is selected on an almost continuous way. Recently, a very wide bandwidth (4 nm) chirped grating has been fabricated [9] which will allow many array antenna elements as well as moderate wavelength tolerances for the lasers. Even though the use of chirped fiber grating has been proposed [6-7], it has not been demonstrated yet, and its continuous group delay, compactness features have not been exploited. As a difference with previous proposed optical feeders for phased-array antennas [3-7] the approach presented in this paper allows any possible antenna elements phase distribution, not just linear phase, making it suitable for advanced phased array features as selective nulling techniques.

The paper is organized as follows. The principle of the TTD scheme is presented in section II. In section III that scheme is demonstrated as well as the impact of the inaccuracies due to the wavelength laser stability and the linearity of the chirped fiber grating on the phased-array performance is considered. Remarks and discussion on the grating-based optical feeder are reported in section IV. Finally, the conclusion is provided in section V.

II. Principle

The transmitting setup of the proposed TTD optical feeder is sketched in figure 1. This beamformer may be considered either as part of a N-element linear phased array or as the elevation or azimuth parts of an N x N separable square phased array. In any case, a wavelength-to-array-element correspondence is used. The output lights of N narrow tuning bandwidth tunable lasers (λ_1 to λ_N) are combined. Further, this multi-wavelength signal is modulated by the radiofrequency signal employing a external electro-optic Modulator (EOM). In this way, all the wavelengths are modulated by the same microwave signal. The different modulated wavelengths pass through an optical circulator to a long (several centimeter) wide bandwidth chirped fiber grating. The resonance position inside the grating, i.e. the reflection point, depends on the wavelength according to the selected chirping law. If a linear chirp is chosen the relation between the reflection position and the wavelength is linear, and so is the round-trip delay. Figure 2 depicts schematically the group delay of a linear chirped grating connected as shown in Figure 1. In figure 2 it may be observed that the shorter the wavelength is, the closer the resonance takes place, and the lower the time delay is. The N delayed modulated optical carriers, λ_1 to λ_N are separated by means of a wavelength-division-multiplexed (WDM) demultiplexer and then passed to each antenna element after photodetection (PD). Depending on the specific values of optical bandwidth and optical carriers separation, the

WDM demultiplexer may implemented as an 1xN optical coupler and N narrowband unchirped grating filters.

The wavelength output of each laser (λ_i) may be tuned around its center position, allowing a relative time delay range of [$-\tau_{MAX}$, τ_{MAX}] as is schematically shown in figure 2. In fact, only N-1 lasers need to be tunable. For a N-element linear antenna, the maximum delay to be implemented is,

$$\tau_{MAX}(ps) = 16.7 * (N-1) * d(cm) * sin(\Theta_{MAX-SCAN}) \qquad (1)$$

where d is the antenna element separation and $\theta_{MAX\text{-}SCAN}$ is the maximum scan angle relative to broadside direction. For broad bandwidth phased array antennas, the typical element spacing is $\lambda_{MIN}/2$, where λ_{MIN} is the microwave wavelength corresponding to the highest frequency. As an example of (1), for a N=10 elements, spaced as d=3 cm, using a maximum RF frequency (f_{RFMAX}) of 5 GHz, and scanning between ±45 degrees, the maximum delay (τ_{MAX}) required is 320 ps. Figure 3 shows the maximum time delay as a function of the maximum scan angle taking f_{RFMAX} and N as parameters. From figure 3, it can be seen that for a maximum delay of ±250 ps at each element, a 6 elements lineal array with a f_{RFMAX} of 2 GHz may be scanned ±25 degrees, and this figure changes to ±35 degrees for N=10 and a f_{RFMAX} of 5 GHz and ±45 degrees for 15 elements and a f_{RFMAX} of 10 GHz.

When all the lasers are tuned to their center wavelengths, the main lobe of the pattern array has to be pointed to broadside direction. The broadside direction would require a zero time delay between all the N antenna elements. Therefore, an extra standard single-mode fiber length (L_i) needs to be added to each antenna element branch in order to compensate for the time delay at the corresponding center position wavelength (λ_i), as shown in figure 1. The value of L_i as a function of the mean grating delay slope δ, the wavelength separation between center positions ($\lambda_i - \lambda_1$) and fiber refractive index (n_o) may be expressed as,

$$L_i(cm) = \delta(ps/nm) * (\lambda_i(nm) - \lambda_1(nm)) * \frac{0.03}{n_o} \quad (2)$$

When the extra fiber lengths are added, the system delay response is no longer a constant positive slope function, but a sawtooth response.

The wavelength excursion needed at any laser depends on the maximum expected time delay and the grating group delay response (ps/nm). For a linear chirped this excursion is,

$$\Delta\lambda(nm) = 33.3 * \frac{(N-1) * d(cm) * sin(\Theta_{MAX-SCAN})}{\delta(ps/nm)} \quad (3)$$

Assuming a separation between adjacent wavelengths of one and a half times the used bandwidth, the maximum number of different-delay addressable antenna elements employing a chirped fiber grating with a total bandwidth $\Delta\lambda_{GRATING}$ is,

$$N_{MAX} = \sqrt{\frac{\Delta\lambda_{GRATING}(nm) * \delta(ps/nm)}{50 * d(cm) * sin(\Theta_{MAX-SCAN})}} \quad (4)$$

where expression a constant group delay slope has been assumed for the whole bandwidth $\Delta\lambda_{GRATING}$.

In order to demonstrate the concept described in section II a four antenna elements phased array has been considered. The experimental setup is illustrated in figure 4, and it corresponds to a single branch of the general scheme shown in figure 1. The fiber grating employed in this experiment is a 40 cm long tapered linearly chirped grating with a linear group delay response over 4 nm ($\Delta\lambda_{GRATING}$ = 4 nm) between 1547 nm and 1551 nm. The mean group delay slope is 835 ps/nm. According to (4) and assuming a ±45 degrees scanning range, this grating would allow a maximum number of elements of 6 for an antenna elements equally spaced with a d of 3 cm. We will assume N=4, d=4cm and a full scanning range (±90 degrees). From (1) and (3) a maximum delay (τ_{MAX}) of 200 ps and a wavelength excursion ($\Delta\lambda$) of nearly 0.5 nm are obtained. The center wavelengths for each laser/element are equally spaced and the following values were chosen λ_1=1547.5 nm, λ_2=1548.5 nm, λ_3=1549.5 nm and λ_4=1550.5 nm. As previously mentioned, these center wavelength will need some compensating fiber length (L_i). Assuming a fiber refractive index (n_0) of 1.46 the theoretical values for these extra lengths are ΔL_1 = 0 cm, ΔL_2 = 17.16, ΔL_3 = 34.32 cm and ΔL_4 = 51.47 cm. The exact L_i values may be obtained from the actual group delay fiber grating response measurements.

In order to show the potential broad bandwidth of the system, and due to its true time delay feature, the group delay measurements were made at four different microwave frequencies, 2, 5, 10 and 18 GHz, covering more than three octaves. The time delay for the full grating bandwidth (1547 nm to 1551 nm) was measured at each microwave frequency.

Once the system time delay response over the full bandwidth $\Delta\lambda_{GRATING}$ is known, two parameters should be extracted for each laser/element system branch. Namely, the mean delay at each center wavelength (relative time delay to λ_1) τ_i, which will be compensated by the corresponding extra fiber length L_i, and the relation between the time delay and the wavelength deviation around λ_i, which is assumed to be linear. This time delay-wavelength deviation is resumed in the slope δ_i at λ_i. Taking into account a 0.5 nm. bandwidth around each λ_i and using a least square linear approximation for all the four radiofrequencies considered, the results shown at Table I were obtained. After compensating the time delay at the center wavelength λ_i, the time delay measurements for each element (around the associated wavelength) for all the four microwave frequencies are obtained as shown in figure 5. In figure 5 it may be observed that the time delay is as expected, i.e. almost linear and independent of the RF frequency. The Pattern Controller shown in figure 1 will use the slope parameter δ_i as reference for each laser tuning. Figure 6 shows the time delay results that will be obtained at each antenna element for an input RF signal of 5 GHz as a function of the steering angle, considering that each tunable laser is driven according to the slope from Table I. The ideal expected results are also shown in figure 6, and it can be seen that the agreement between the theoretical (ideal) and the experimental results are excellent. The rms error is given in Table II. The ripple around the ideal linear grating group delay response will introduce some error which should be considered for the system performance evaluation, but this is not the only cause of error. The total system time delay error should be estimated assuming two main causes of error: the laser wavelength stability $\Delta\lambda_{LASER}$, and the fiber grating time delay response deviation from the linear slope $\sigma_{GRATING\text{-}SLOPE}$. The laser wavelength stability can be translated to time precision by taking into account the grating response around each λ_i as,

$$\sigma_{LASER}(\lambda_i) = \Delta\lambda_{LASER} * \delta_i \qquad (5)$$

The $\sigma_{GRATING\text{-}SLOPE}$ parameter must be estimated over the full needed bandwidth, (0.5 nm. from (3)), around each center wavelength, and the standard deviation of the measurements from the linear approximation (slope δ_i at each λ_i) is calculated. Table II shows the results extracted from the measurements for all four wavelength and for all four microwave frequencies. The mean standard deviation for each microwave frequency is also given. A total standard deviation of 3.31 ps would resume the time delay uncertainty due to the grating group delay ripple. Taking into account both effects, laser wavelength stability and the grating response, a total system precision can be estimated as,

$$\sigma^2_{TOTAL}(\lambda_i, f_{RF}) = \sigma^2_{LASER}(\lambda_i) + \sigma^2_{GRATING-SLOPE}(\lambda_i, f_{RF}) \quad (6)$$

The results for σ_{TOTAL} assuming a laser wavelength stability of 0.01 nm are shown in Table III. According to these results, the total system time delay precision is 8.94 ps, which in turn implies a time delay equivalent to a 16.1 degrees phase error at 5 GHz or 6.44 degrees at 2 GHz. These results are similar to the precision of a 3.5 bits microwave digital phase shifter operating at 5 GHz, or a 5 bits microwave digital phase shifter operating at 2 GHz.

In this experiment the time delay error comes mainly due to the laser wavelength stability. Therefore, just a little improvement in the laser wavelength stability will yield impressive results. For instance a laser stability reduction to half its value ($\Delta\lambda_{LASER}$ = 0.005 nm) provides a total time delay rms error value of 5.31 ps, which is equivalent to a 3.8 degrees phase rms error operating at 2 GHz (almost a 6 bits microwave phase shifter resolution).

In a second experiment we insert 23 km of standard single-mode fiber between the optical circulator and the EOM, which results in converting the system dispersion of the 835 ps/nm grating in an equivalent grating with a dispersion of 430 ps/nm. The main effect of the equivalent dispersion change on the scheme is to provide a broader bandwidth $\Delta\lambda_i$ for the same maximum time delay τ_{MAX} , and thus the sensitivity of the laser wavelength stability is reduced. Assuming an array antenna with N = 4, d = 4 cm and a ±45 degrees scanning angle, a maximum delay (τ_{MAX}) of 140 ps and a wavelength excursion ($\Delta\lambda$) nearly 0.65 nm are obtained from (1) and (3). The measurements were made only for a microwave frequency of 2 GHz. The results (L_{i}, δ_i, σ_{TOTAL}, $\sigma_{GRATING\text{-}SLOPE}$) are summarized in Table IV. The corresponding time delay measured responses at each center wavelength λ_i are shown in figure 7. As expected, the total rms time error for a laser wavelength stability of 0.01 nm is reduced to 5.3 ps., which is equivalent to a 3.8 degrees rms phase error at 2 GHz, as a result of the reduced slope of the time delay response. On the other hand, a broader bandwidth is required than that in the previous experiment, which will impact on reducing the maximum number of elements of the array for a fixed full grating bandwidth.

IV. Remarks and Discussion

The results obtained and presented in section III confirm the expected good performance employing the proposed optical beamforming scheme. That results may be even improved with specifically tailored fiber gratings, which should be more focused on achieving very low group delay response ripple instead of a highly linear response as required for dispersion compensation applications. Opposed to previously proposed optical beamformers that employ only one broad bandwidth tunable laser [4], or several fixed multiwavelength sources [3], the phase pattern at the antenna elements plane is not limited to the linear phase one. For a particular phased array antenna application in which a linear phase distribution is specified, the system requirements are reduced, as the maximum time delay for each element is no longer the same, but depending on the element position to antenna geometrical center. Therefore, the associated optical bandwidth ($\Delta\delta_i$) is different for each element and it is not necessary to be designed for the worst case as in the simple experiment here shown.

The effect of the N tunable lasers on the overall system cost is not dramatic because of the lasers do not require a broad tuning bandwidth, but just tenths of a nanometer, which should reduce its cost. The use of just one grating for the whole system is a clear advantage compared to previous true time delay schemes proposed since mismatches in the numerous gratings may result in important inaccuracies.

The laser wavelength stability has been proved to have a very high effect on the whole system performance, and its reduction will be a very important issue for the development of future beamformers.

The maximum number of antenna elements for the proposed beamformer is currently limited to few tens for frequencies between L-Band an X-band, but the available fiber grating lengths are growing from one day to the other, so the 40 cm long fiber grating employed in the experiment will be considered short in a few months. Furthermore, the group delay gratings response employed in our approach is by no means limited to a linear behavior as it is for dispersion compensating applications. The more stringent requirement is the ripple in the delay response. Some other group delay responses are currently under study.

The dispersion-generated time delay is accompanied by dispersion-induced signal distortion as it is in the previously proposed systems using very long dispersive fiber lengths [3-5], but the wide bandwidth chirped grating fiber allows a huge reduction in size.

V. Conclusion

To the best of our knowledge, the first demonstrated continuous true-time-delay beamforming with wide bandwidht chirped grating, suitable for arbitrary antenna element phase distribution. A 40 cm long chirped fiber grating has been used as the only dispersive element of the system, and it has been proved to potentially drive a 4 elements wide-bandwidth phased array with high resolution (6 bits) at L and S bands. Inaccuracies due to the wavelength stability of lasers and the linearity of the chirped grating group delay have been also considered and their impact on the phased-array performance is reported.

Acknowledgments: The authors wish to thank the Spanish Research Commission (CICYT) for funding the project TIC96-0611. This work was partially supported by Pirelli Cavi SpA. The grating technology were developed as part of a collaborative project between Pirelli Cavi SpA and South

References

[1] A. Seeds, "Optical Technologies for Phased Array Antennas", IEICE Trans. Electron., vol. E76-C, 2, pp.198-206, 1993.

[2] T. Berceli, W.Jemison, P.R. Herczfeld, A.S. Daryoush, A. Paolella, "A Double-Stage Injection-Locked Oscillator for Optically Fed Phased Array Antennas", IEEE Trans. Microwave Theory and Tech., 39, 2, pp.201-208, 1991.

[3] Tong, D.T.K. and Wu, M.C. “A novel multiwavelength optically controlled phased array antenna with a programmable dispersion matrix”. *IEEE Photon. Tech. Letters*, 8, pp. 812-814, 1996.

[4] R.D. Esman, et al. “Fibre-optic prism true time-delay antenna feed”. *IEEE Photon. Tech. Letters*, 5, pp. 1347-1349, 1993.

[5] M.Y. Frankel, P.J. Matthews, R.D. Esman “Two-Dimensional Fiber-Optic Control of a True Time-Steered Array Transmitter”. 1996 IEEE MTT-Symposium Digest, pp. 1577-1580.

[6] D.T.K. Tong, M.C Wu, “Programmable dispersion matrix using Bragg fibre grating for optically controlled phased array antennas”. *Electronics Letters*, 32, pp. 1532-1533, 1996.

[7] A. Molony et al. “Fibre grating time delay element for phased array antennas”. *Electronics Letters*, 31, 1485-1486, 1995.

[8] R.A. Soref, “Fiber grating prism for true time delay beamsteering”. *Fiber and Integrated Optics*,15, pp.325-333, 1996.

[9] M.J. Cole, H. Geiger, R.I. Laming, S.Y. Set, M.N.Zervas, W.H. Loh, V.Gusmeroli, "Continously chirped, broadband dispersion-compensating fibre gratings in a 10 Gbits/s 110 km standard fibre link", 22nd European Conf. Optical Comm., Oslo, paper ThB.3.5, 1996.

Figure Captions

Figure 1. TTD Beamformer Transmitting Mode Block Diagram.

Figure 2. Fiber grating group delay response and nominal wavelengths placement, showing available wavelength excursion.

Figure 3. Maximum time delay as a function of scanning angle from broadside for different combinations of number of elements (N) and antenna spacing (d).

Figure 4. Experiment setup for characterizing the relative time delays of one single branch of the TTD beamformer.

Figure 5. Time Delay measurements at each antenna element for four different microwave frequencies (2,5,10 and 18 GHz) as a function of deviation from central wavelength ($\Delta\lambda$). Each figure corresponds to a different wavelength. The grating dispersion is 835 ps/nm.

Figure 6. Time delay measurements (dashed lines) and theoretical results (solid lines) as a function of the scan angle when f_{RF} = 5 GHz.

Figure 7. Time Delay measurements at each antenna element at 2 GHz. as a function of deviation from central wavelength ($\Delta\lambda$) for a different grating slope (430 ps/nm).

Table captions

Table I. RMS Time Delay and Slope at each central wavelength for four different microwave frequencies, assuming a 0.5 nm bandwidth.

Table II. Time delay standard deviation from the linear response (δ_i).

Table III. Total RMS time delay error, taking into account the grating group delay response and the laser wavelength stability.

Table IV. Results summary for the 430 ps/nm equivalent grating.

TABLE I

λ_i (nm.)	Mean Relative Time Delay (ps.) at λ_i	Compensating Length, L_i (cm.)	Slope δ_i (ps./nm.)
1547.5	**0**	**0**	**787**
1548.5	**824.1**	**16.93**	**819**
1549.5	**1653.7**	**33.98**	**850**
1550.5	**2505.8**	**51.49**	**865**

TABLE II

$\sigma_{GRATING\ SLOPE}$	λ_1 1547.5 nm.	λ_2 1548.5 nm	λ_3 1549.5 nm.	λ_4 1550.5 nm.	Mean σ
2 GHz	**3.87 ps.**	**3.83 ps.**	**2.90 ps.**	**4.04 ps.**	**3.69 ps.**
5 GHz	**2.81 ps.**	**3.37 ps.**	**2.49 ps.**	**2.53 ps.**	**2.82 ps.**
10 GHz	**3.02 ps.**	**2.99 ps.**	**2.01 ps.**	**2.27 ps.**	**2.61 ps.**
18 GHz	**2.59 ps.**	**2.35 ps.**	**3.39 ps.**	**6.17 ps.**	**3.93 ps.**

TABLE III

σ_{TOTAL}	λ_1 1547.5 nm.	λ_2 1548.5 nm	λ_3 1549.5 nm.	λ_4 1550.5 nm.	Mean σ
2 GHz	**8.77 ps.**	**9.05 ps.**	**8.98 ps.**	**9.55 ps.**	**9.09 ps.**
5 GHz	**8.35 ps.**	**8.86 ps.**	**8.86 ps.**	**9.01 ps.**	**8.77 ps.**
10 GHz	**8.42 ps.**	**8.72 ps.**	**8.73 ps.**	**8.94 ps.**	**8.71 ps.**
18 GHz	**8.28 ps.**	**8.51 ps.**	**9.15 ps.**	**10.6 ps.**	**9.19 ps.**

TABLE IV

λ_i (nm.)	Compensating Length, L_i (cm.)	Slope δ_i (ps./nm.)	$\sigma_{GRATING\ SLOPE}$	σ_{TOTAL}
1547.5	**0**	**396**	**3.27 ps.**	**5.13 ps.**
1548.5	**8.63**	**416**	**3.58 ps.**	**5.49 ps.**
1549.5	**17.31**	**449**	**2.45 ps.**	**5.12 ps.**
1550.5	**26.59**	**463**	**3.11 ps.**	**5.58 ps.**

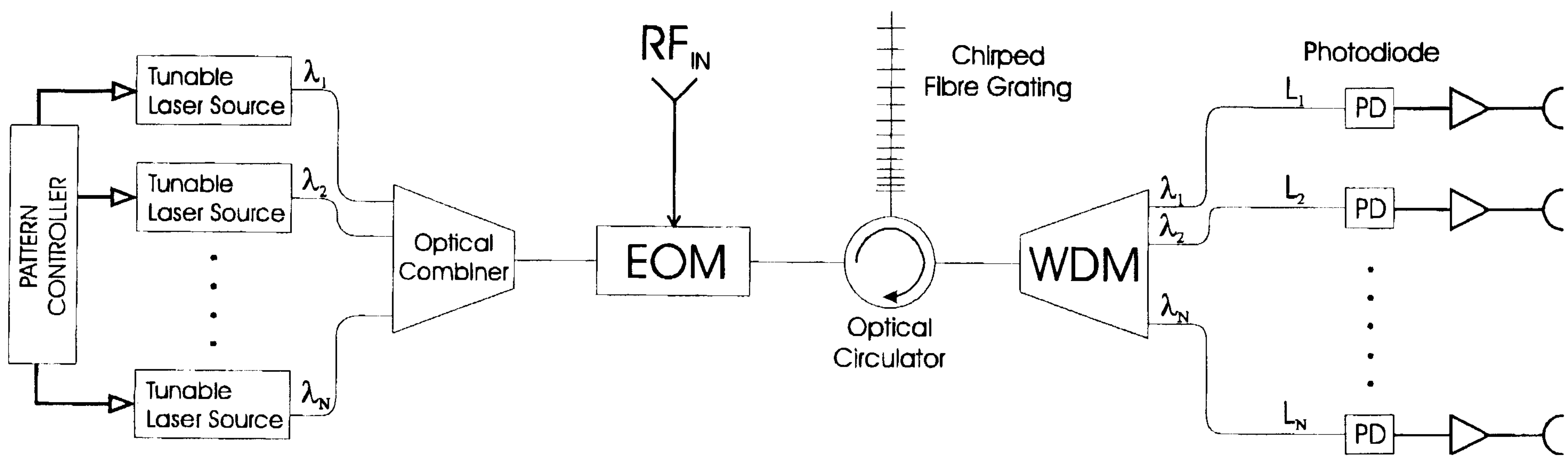
PATTERN CONTROLLER
Tunable Laser Source
Tunable Laser Source
Tunable Laser Source
λ_1
λ_2
λ_N
Optical Combiner
RF_{IN}
EOM
Chirped Fibre Grating
Optical Circulator
WDM
λ_1
λ_2
λ_N
Photodiode
L_1
L_2
L_N
PD
PD
PD

Figure 1

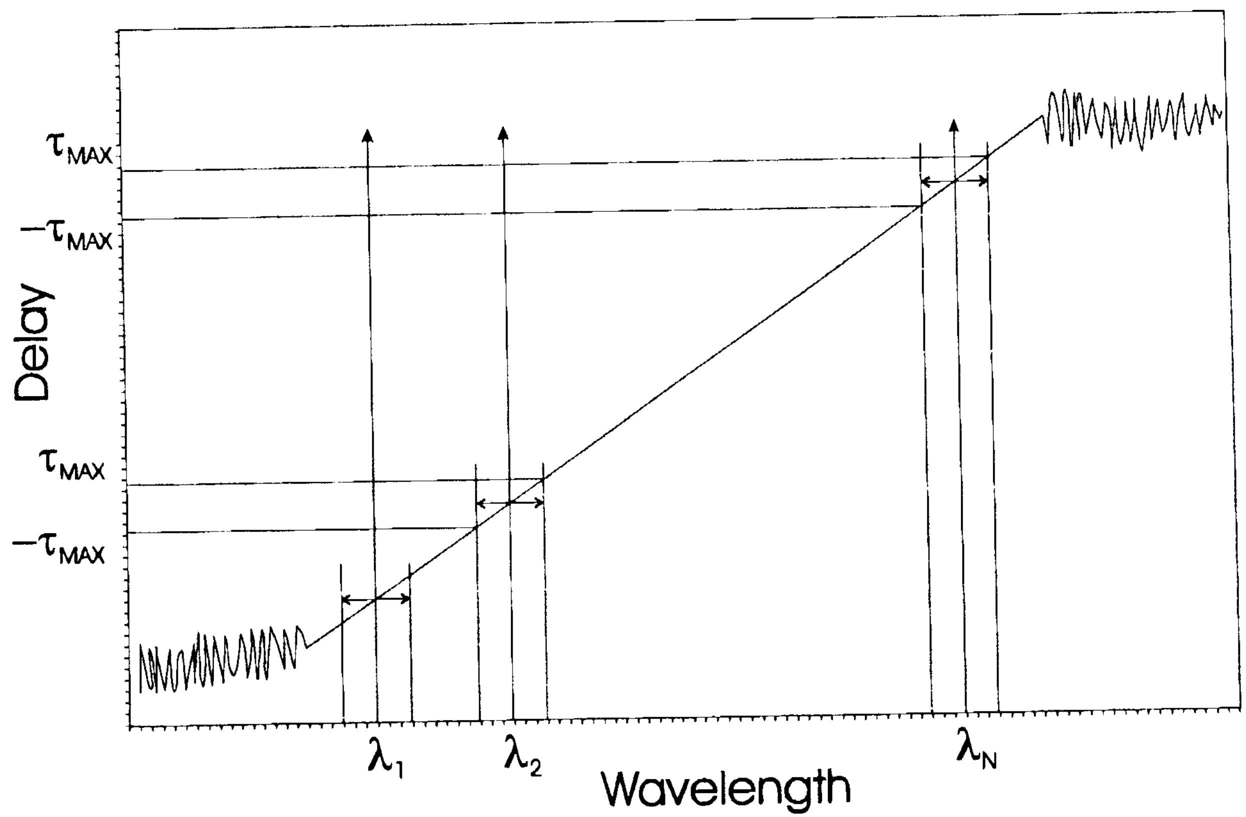

Delay
τ_{MAX}
$-\tau_{MAX}$
τ_{MAX}
$-\tau_{MAX}$
λ_1
λ_2
λ_N
Wavelength

Figure 2

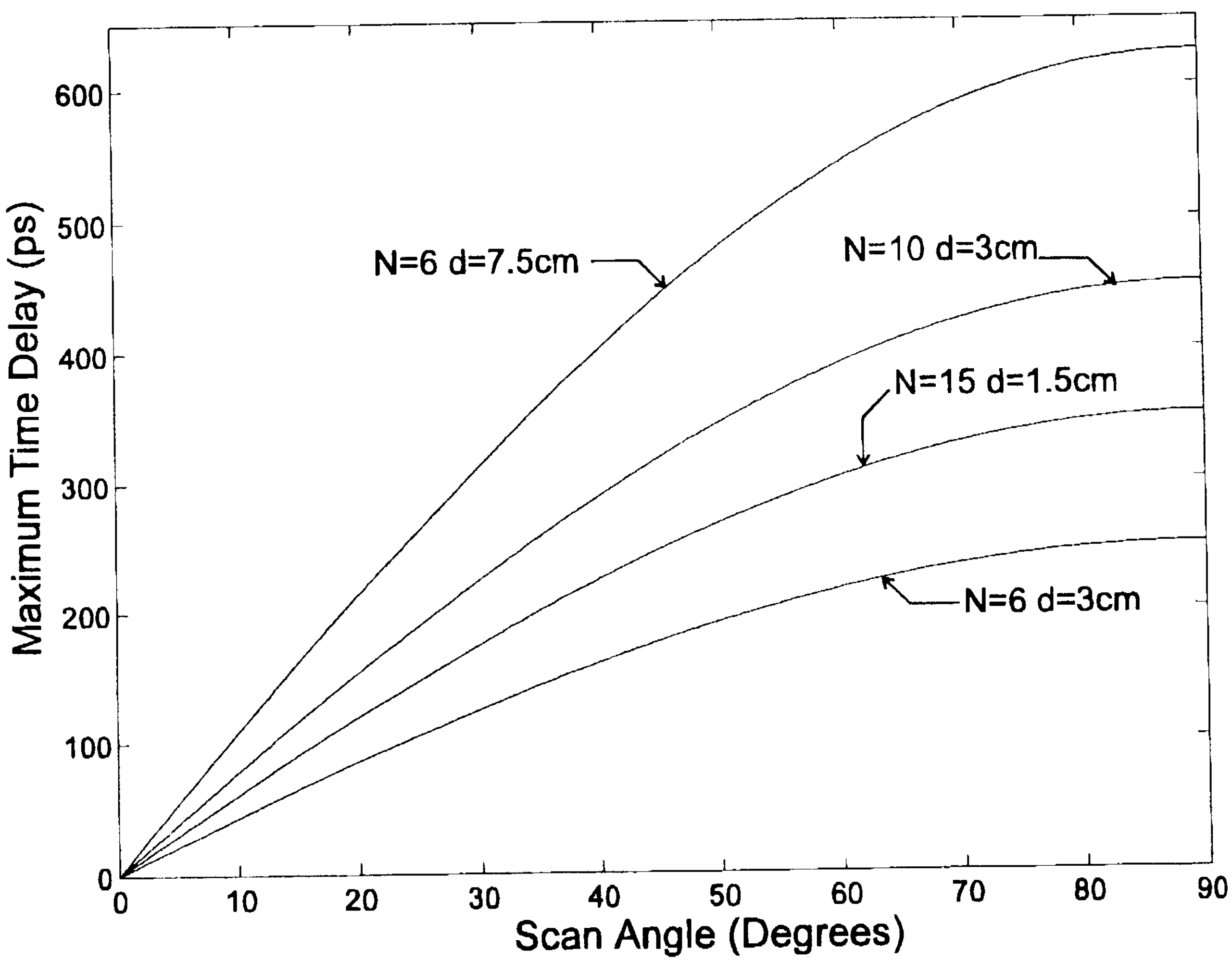
Maximum Time Delay (ps)
600
500
400
300
200
100
0
0
10
20
30
40
50
60
70
80
90
Scan Angle (Degrees)
N=6 d=7.5cm
N=10 d=3cm
N=15 d=1.5cm
N=6 d=3cm

Figure 3

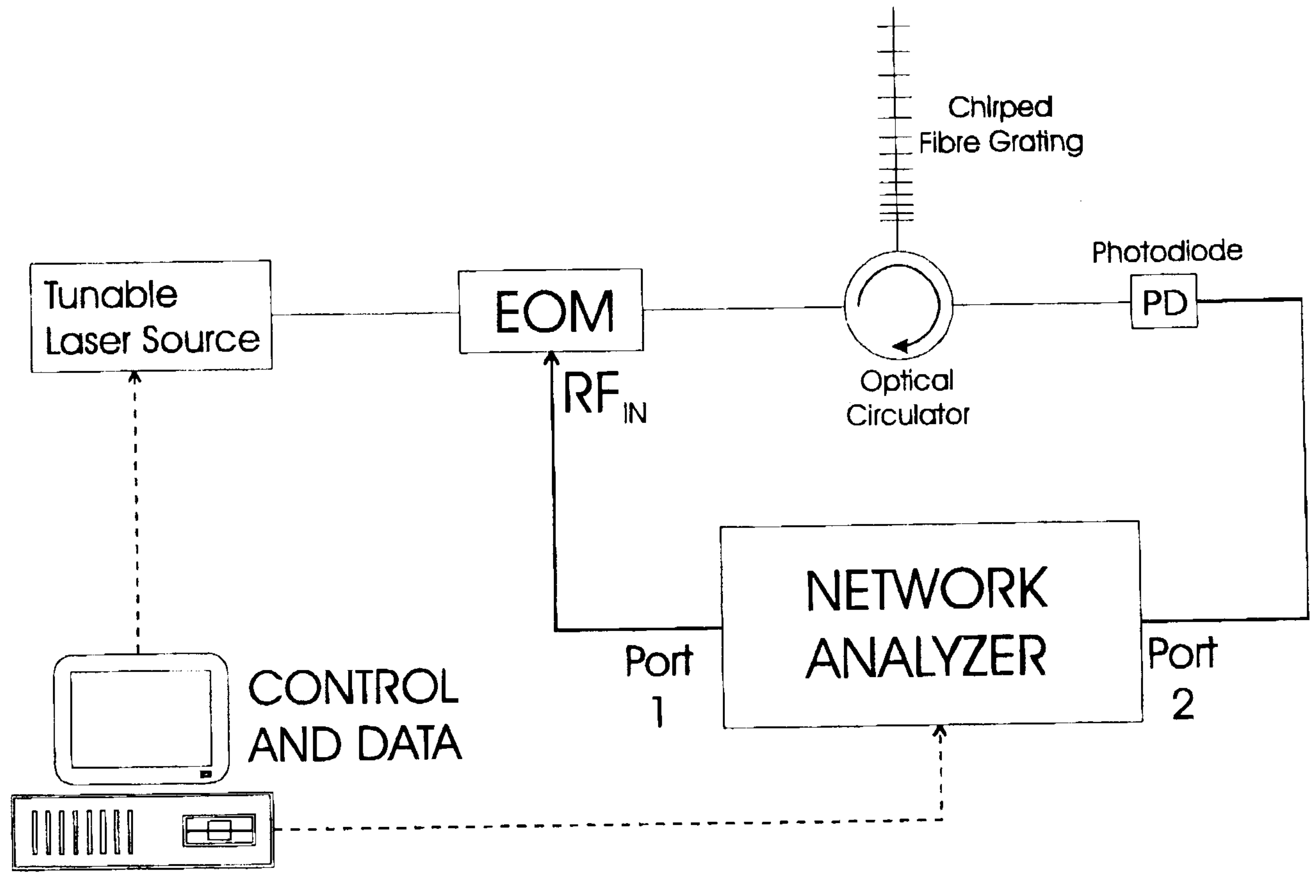
Tunable
Laser Source
EOM
RF IN
Chirped
Fibre Grating
Optical
Circulator
Photodiode
PD
CONTROL
AND DATA
NETWORK
ANALYZER
Port
1
Port
2

Figure 4

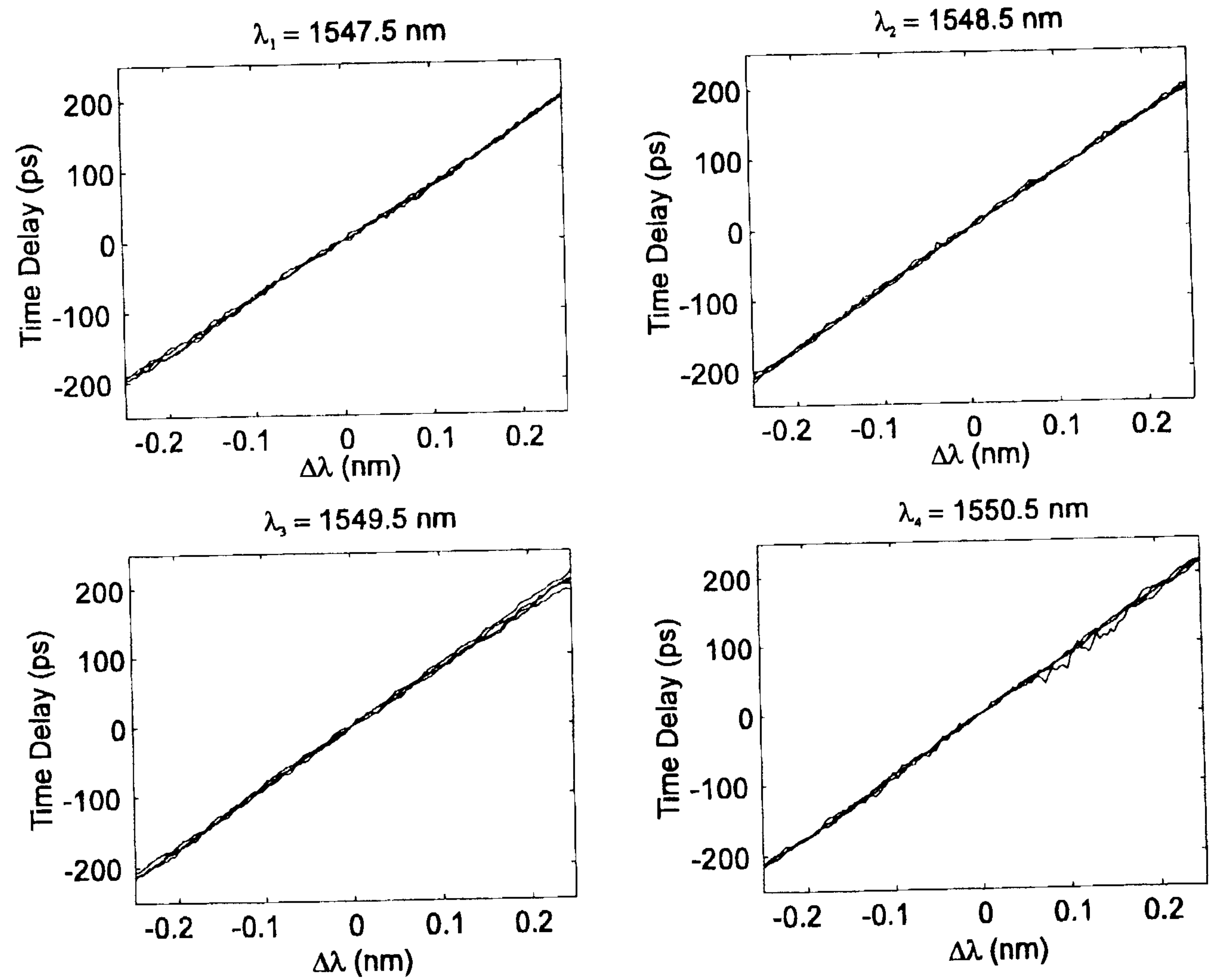

λ_1 = 1547.5 nm
λ_2 = 1548.5 nm
λ_3 = 1549.5 nm
λ_4 = 1550.5 nm
Time Delay (ps)
200
100
0
-100
-200
-0.2
-0.1
0
0.1
0.2
Δλ (nm)

Figure 5

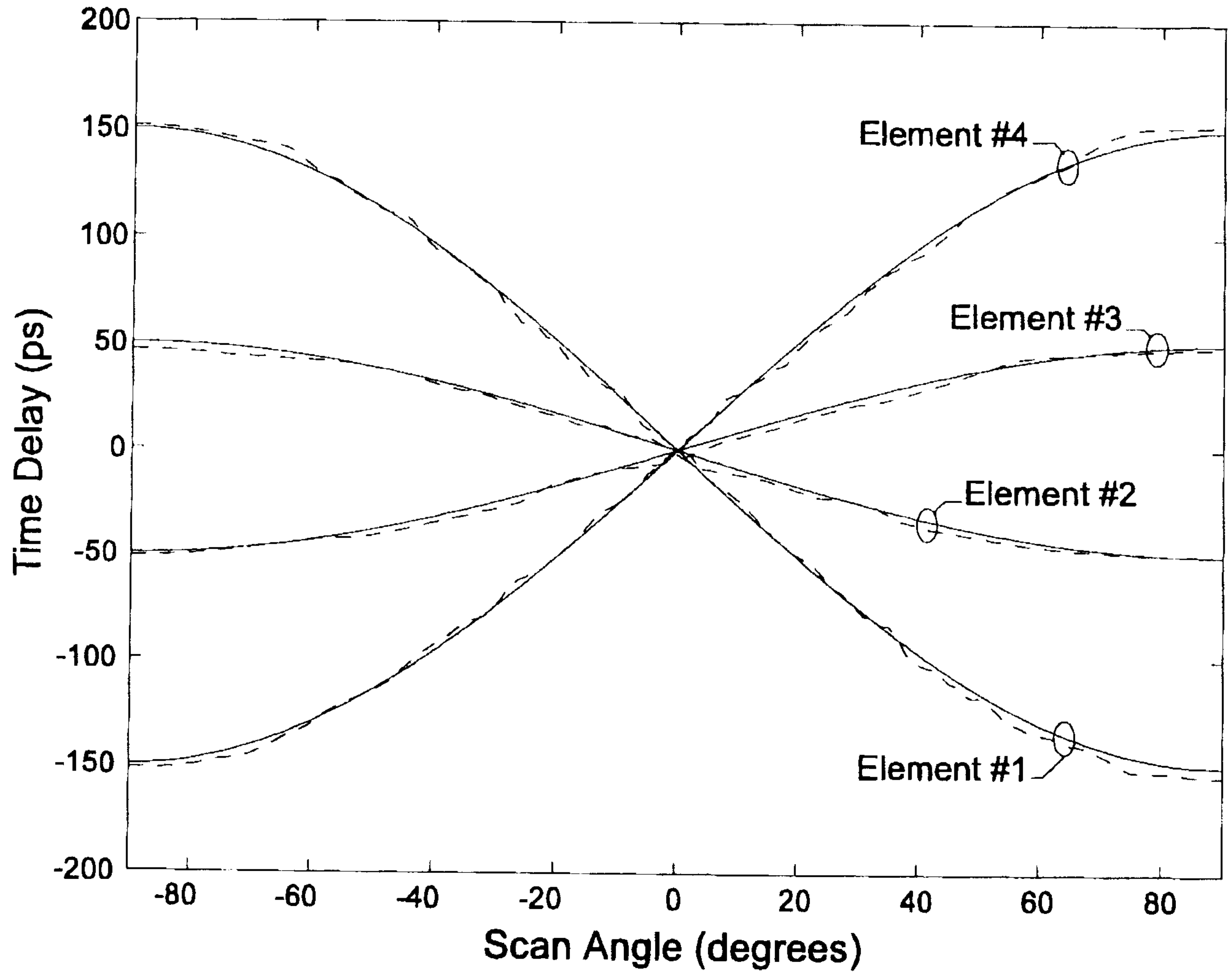
Time Delay (ps)
200
150
100
50
0
-50
-100
-150
-200
Scan Angle (degrees)
-80
-60
-40
-20
0
20
40
60
80
Element #4
Element #3
Element #2
Element #1

Figure 6

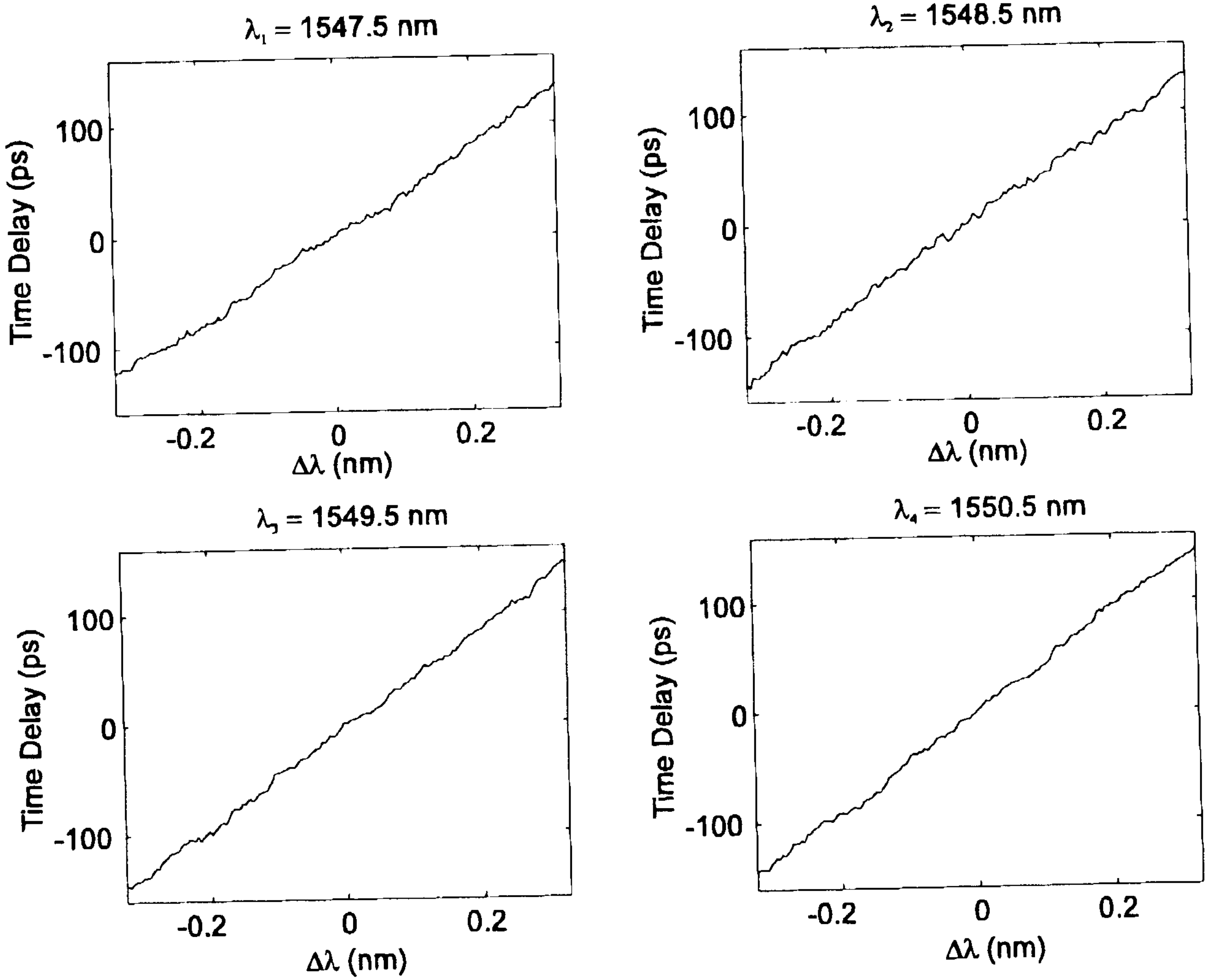
λ_1 = 1547.5 nm
λ_2 = 1548.5 nm
λ_3 = 1549.5 nm
λ_4 = 1550.5 nm
Time Delay (ps)
100
0
-100
-0.2
0
0.2
Δλ (nm)

Figure 7